Analyst

Accepted Manuscript

ROYAL SOCIETY OF CHEMISTRY

www.rsc.org/analyst

Analyst

PAPER

Electrochemical monitoring of colloidal silver nanowires in aqueous samples

Received 00th January 20xx,
Accepted 00th January 20xx

DOI: 10.1039/x0xx00000x

www.rsc.org/

Cheng Ai Li and Duckjong Kim*

Silver nanowires (NWs) are increasingly utilized in technological materials and consumer products, but an effective analytical technique is not yet available to measure their concentration in the environment. Here, we present an electrochemical method to quantify Ag NWs suspended in aqueous solution. Using linear sweep voltammetry, the Ag NWs are identified by the peak potential while their concentration is revealed by the intensity of the peak current. The peak current varies linearly with the Ag NW concentration with a low detection limit of 3.50 ng·mL^{-1}. This method is also successfully applied to quantify Ag NWs in mixtures with nanoparticles, through their specific oxidation behavior, and in wastewater obtained after Ag NW film preparation process.

Introduction

The highly desirable electrical, mechanical, and optical properties of Ag nanowires (NWs) have recently been exploited to prepare transparent flexible electrodes,[1] and they are also utilized in optoelectronic devices such as liquid crystal displays, solar cells, light emitting diodes.[2-5] However, the toxicity of Ag NWs makes their increasing production and release into the environment a cause of great concern. Verma et al. found Ag NWs to be mildly cytotoxic to four different cell lines, the toxicity varying with the cell type, nanowire length, dose, and incubation time.[6] In studying the toxicity of Ag NWs to *Escherichia coli*, Visnapuu et al. observed that the 4-hour median effective concentration (EC_{50}) was 0.42 ± 0.06 μg·mL^{-1}.[7] Scanlan et al. investigated the acute toxicity of different-sized and coated Ag NWs on Daphnica magna, classifying poly(vinylpyrrolidone)-coated Ag NWs as highly toxic, with 24 h median lethal concentrations (LC_{50}) ranging from 0.2339 to 0.4210 μg·mL^{-1} in simulated freshwater media.[8] Since previous studies have associated the toxicity of silver nanomaterials with the release of silver ions (Ag^+) from their surface,[7,9] considerable research efforts have been devoted to sensitive detection methods for Ag^+.[10] However, Ag NWs in aquatic environments are intrinsically toxic to organisms.[6,8,11] Kim and Shin showed that Ag NWs rather than the Ag ions mainly cause rheological changes of human blood from their controlled experiment.[11] A suitable analytical technique is therefore required to quantify Ag NWs directly. Some techniques have been proposed to measure the concentrations of metallic nanomaterials.[12-14] However, these systems involve costly and complex optics and are difficult to miniaturize into inexpensive portable instruments for on-site analysis.

In contrast, an electrochemical method potentially offers rapid and sensitive analyte determination with a more cost-effective and portable setup. In this approach, electrical signals (e.g. current, potential, charge and impedance) associated with chemical reactions are measured using an electrochemical cell.[15-19] The most commonly used electrochemical cell consists of working, reference, and counter electrodes in an electrolyte solution. This simple and inexpensive setup is widely employed for industrial or environmental analysis. Recently, the electrochemical method was applied to detection of Ag nanoparticles (Ag NPs). However, it has seldom been used to quantify Ag NWs. Here, we have adopted an adsorption and electrochemical detection as shown in scheme 1. We immerse clean glassy carbon (GC) electrodes (3 mm in diameter) into a solution containing Ag NWs, leading to their adsorption to the rod. The resulting coverage depends on the concentration of Ag NWs in the solution. The adsorbed NWs are subsequently stripped from the electrode by linear sweep voltammetry (LSV). When the potential applied to the electrochemical cell reaches the oxidation potential of Ag NWs, Ag NWs adsorbed on the

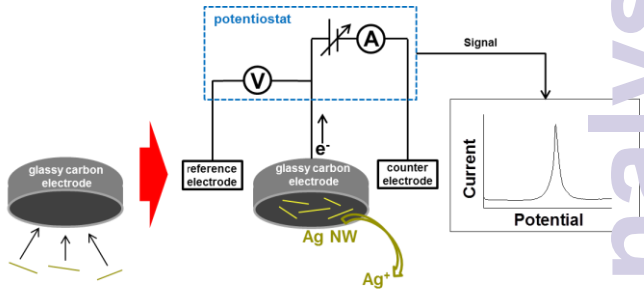

Scheme 1. Method for electrochemical detection of Ag NWs in aqueous solution.

Department of Nano Mechanics, Korea Institute of Machinery and Materials, 171 Jang-dong, Yuseong-gu, Daejeon 305-343, Republic of Korea.
E-mail: dkim@kimm.re.kr.

electrode is oxidized and the current response according to the oxidation is detected. This oxidation results in a current peak, the magnitude of which is determined by the number of Ag NWs on the electrode surface; this in turn is proportional to the NW concentration in the solution.

Experimental

Chemicals

All reagents were of analytical grade. Two kinds of Ag NWs (1 wt%, 20–30 nm diameter, 10–20 µm length; 1 wt%, 40–60 nm diameter, 15–25 µm length) and Ag NPs (3 wt%, ~51.3 nm diameter) were purchased from Ditto Technology (Anyang, South Korea) as suspensions in water, which were diluted and sonicated for 5 min before use. Sodium perchlorate was purchased from Sigma, diluted in ultrapure water (resistivity ≥ 18.2 MΩ·cm, Millipore), and degassed thoroughly with N_2.

Materials characterization

The Ag NWs and NPs were characterized using a scanning mobility particle sizer (TSI 3080), scanning electron microscopy (SEM, FEI Nova NanoSEM 200; acceleration voltage, 10 kV), and powder X-ray diffraction (XRD, PANalytical Empyrean Series 2; Cu-Kα radiation, λ = 0.154060 nm).

Electrochemical analysis

Voltammetric measurements were carried out with a CHI 660E analyzer connected to a three-electrode arrangement, with a NaCl reference electrode (BASi company, USA), a Pt auxiliary electrode, and a glassy GC working electrode (3 mm in diameter), from 0 to 0.6 V vs. [3 M] Ag/AgCl/Cl^-. The electrochemical cell was filled with 25 mL of 0.1 M $NaClO_4$ as the background electrolyte to obtain the voltammograms with the GC electrode. All the electrochemical measurements were performed in triplicate at least, with new solutions and glassware in each case. The NW–NP mixture voltammograms were fit using Origin v.8.6 to separate the two oxidation peaks.

Preparation of Ag NW films and concentration measurement

Ag NW films were prepared by vacuum drawing Ag NW suspensions through porous mixed cellulose ester membranes (0.45 µm, 47 mm); the films were then dried at room temperature. The Ag concentration in the filtrate was measured in triplicate by inductively coupled plasma optical emission spectrometry (ICP-OES, Agilent, ICP-OES 720) after acid digestion.

Results and discussion

The procedure used to measure the solution concentration of Ag NWs was as follows. First, the GC electrode was subjected to mechanical polishing and cyclic voltammetric scanning using a 0.1 M $NaClO_4$ electrolyte to ensure that there is no pre-adsorbed material. The working electrode was then transferred to freshly prepared solutions with different Ag NW contents, which were sonicated for 5 min to disperse the nanowires homogeneously. After immersing the electrode for

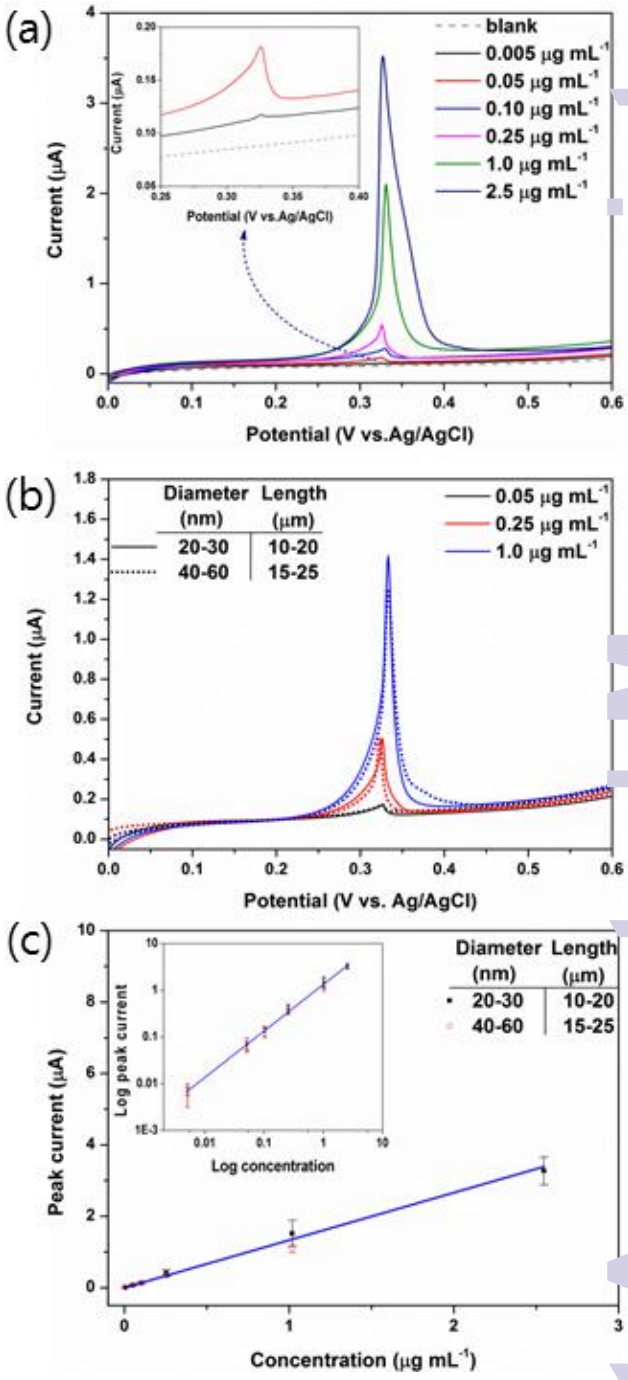

Fig. 1 (a) Linear sweep voltammograms of Ag NWs (D = 20-30 nm, L = 10-20 µm) at 0.005, 0.05, 0.10, 0.25, 1.0, 2.5 µg·mL^{-1} in 0.1 M $NaClO_4$, recorded at a scan rate of 20 mV·s^{-1}. The inset shows higher magnification voltammograms of a blank control and of solutions containing 0.005 and 0.05 µg·mL^{-1} Ag NWs. (b) Linear sweep voltammograms of two kinds of Ag NWs (D = 20-30 nm, L = 10-20 µm; D = 40-60 nm, L = 15-25 µm) at 0.05, 0.25, 1.0 µg·mL^{-1} in 0.1 M $NaClO_4$, recorded at a scan rate of 20 mV·s^{-1}. (c) Calibration curve used to relate the peak current to the concentration of Ag nanowires. The inset shows the same data on logarithmic scales.

10 min, the Ag NW suspension was characterized by LSV. As shown in the inset of Fig. 1a, the linear sweep voltammogram of the GC electrode shows no anodic peak in the absence of Ag NWs, while for the electrolyte containing Ag NWs, a well-defined oxidation peak appears at ~0.33 V vs. Ag/AgCl, consistent with the one-electron oxidation of metallic Ag^0 to Ag^+.[21] During LSV scanning, the magnitude of the current signal originating from an electrochemical cell reflects the activity or concentration of the analytes in the cell. The peak potential can be used to identify unknown species while the intensity of the peak current gives their concentration.

Fig. 1a shows linear sweep voltammograms of a GC electrode placed in solutions with different concentrations of Ag NWs (D = 20-30 nm, L = 10-20 μm). The intensity of the peak current increases with the concentration of Ag NWs as more of these become attached to the electrode. The effect of Ag NW size on its oxidation was also investigated by detecting Ag NWs having different diameter and length (D = 40-60 nm, L = 15-25 μm). Fig 1b shows that the larger Ag NWs are detected in the same peak potential and that the effect of the Ag NW size on the peak current according to the concentration is insignificant. There have been some reports showing the size dependency of the oxidation potential for Ag NPs with diameter smaller than 25 nm.[22,23] Even though we have not seen any evidence of the size effect for Ag NWs whose diameter is larger than 20 nm, the size effect for extremely thin Ag NWs requires further study. A quantitative relationship between the peak current and the Ag NW concentration was derived, as shown in Fig. 1c. The peak intensity from silver oxidation depends linearly on the Ag NW concentration from 0.005 to 2.5 $\mu g \cdot mL^{-1}$. The equation obtained by linear regression for these data was I (μA) = 0.00017 + 1.331 C ($\mu g \cdot mL^{-1}$)—where I and C are the peak current and the AgNW concentration, respectively—with a linear regression coefficient R^2 = 0.991. The estimated detection limit was 3.50 $ng \cdot mL^{-1}$ at a signal-to-noise ratio of 3. This was calculated as 3 times (for a 99.9% confidence level) the standard deviation of the blank measurement divided by the slope of the calibration curve.[24,25] This detection limit is two orders of magnitude lower than the previously reported EC_{50} or LC_{50} values for Ag NWs in aquatic organisms,[7,8,26] and should allow the detection of Ag NWs under environmentally relevant conditions of typically very low concentration. Moreover, the simplicity of this electrochemical method, requiring no complex analytical procedure or multi-step sample preparation, should make on-site Ag NW monitoring possible.

The presence of Ag NPs in the samples was also investigated. Single, well-defined anodic peaks are observed in the voltammograms recorded during electrochemical oxidation of Ag NPs and NWs at different concentrations (Fig. 2a,b). The peak potential for the NWs occurs at a more positive voltage with the difference of ~48 mV. Fig. 2c,d show the voltammograms obtained for mixture

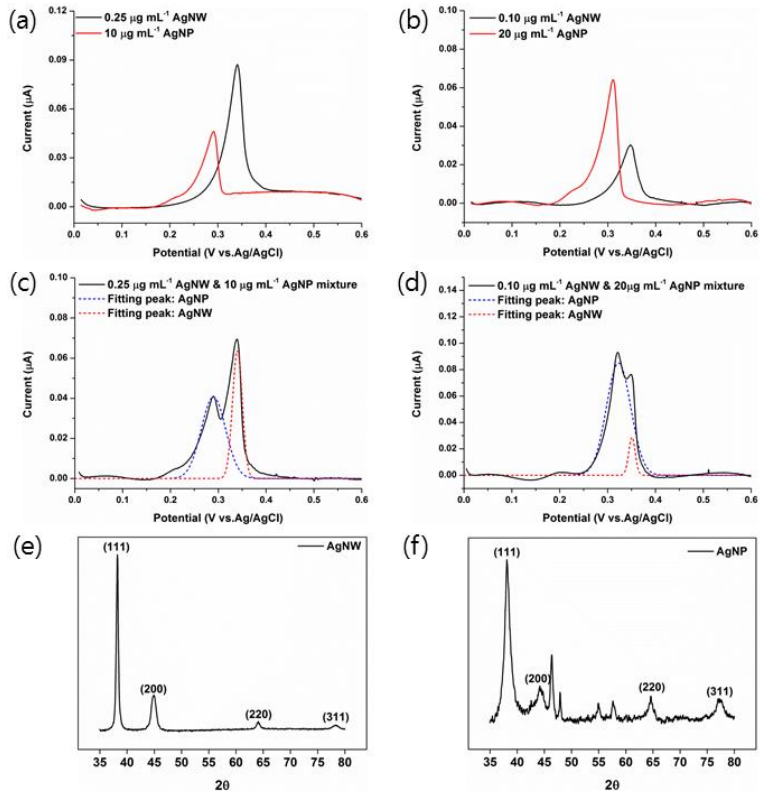

Fig. 2 (a–d) Linear sweep voltammograms (after baseline correction) measured for Ag nanowires (NWs) and nanoparticles (NPs) in 0.1 M $NaClO_4$ at a scan rate of 20 $mV \cdot s^{-1}$; (a) 0.25 $\mu g \cdot mL^{-1}$ NWs (black line) and 10 $\mu g \cdot mL^{-1}$ NPs (red line), (b) 0.10 $\mu g \cdot mL^{-1}$ NWs (black line) and 20 $\mu g \cdot mL^{-1}$ NPs (red line), (c) a 0.25 $\mu g \cdot mL^{-1}$ NW and 10 $\mu g \cdot mL^{-1}$ NP mixture (black line), and (d) a 0.10 $\mu g \cdot mL^{-1}$ NW and 20 $\mu g \cdot mL^{-1}$ NP mixture (black line). Gaussian fits of the NP and NW peaks in the mixture data are respectively shown in blue and red dotted lines. (e, f) X-ray diffractograms of (e) Ag NWs and (f) Ag NPs.

solutions containing different concentrations of Ag NWs and NPs, along with Gaussian deconvolutions of the anodic peaks into NW and NP contributions. These results indicate that the presence of Ag NPs does not noticeably alter the oxidation potential of the NWs. The peak current intensities obtained from the fits (listed in Table 1) agree with those obtained from Fig. 2a,b within the uncertainty associated with each value.

The shape of metal nanomaterials is known to influence their optical and electrical properties,[27-30] while their electrochemical oxidation potential is dependent on their structure.[31] Furthermore, different crystal planes are well known to have different surface energies; this may affect the electrochemical behavior of the Ag NWs and NPs. The XRD patterns recorded for the Ag NWs and NPs, shown respectively in Fig. 2e and f, consist mainly of sharp peaks at 2θ values of ~38°, ~44°, ~64°, and ~78°, respectively arising from the (111), (200), (220), and (311) planes of face centered cubic (fcc) metallic Ag[32-35] (the other weaker peaks in the NP diffractogram are attributed to crystallographic impurities). These XRD data therefore indicate that these NWs and NPs are crystalline. The ratio of the intensities of the (111) and (220) peaks is much higher for the Ag NWs (17.3 vs. 5.1), suggesting that (111) facets are more abundant in the NWs. These ratios are similar to those reported elsewhere for Ag NPs (~4.4) and NWs (~17.3).[31-33] In terms of their surface energy, fcc facets are usually ordered as follows: (111) < (100) < (110).[36] For Ag, the close-packed (111) plane is the crystal plane with the lowest energy, and is therefore the most stable. Since (111) facets are more abundant in the Ag NWs, the NWs are more stable than the NPs, and consequently, their oxidation potential is more positive. In summary, these experimental results indicate that the dissimilar morphologies of Ag NPs and NWs lead to a difference in oxidation potential, which allows their separate quantification using the electrochemical method, as shown in Fig. 2c,d. Furthermore, the electrochemical method described here could be employed to selectively detect Ag NWs against other metallic NPs such as Au, Ni and Cu, due to their different oxidation potentials. The electrochemical oxidation potential of Ag NWs is ~0.33 V vs. Ag/AgCl, which is quite different from the oxidation potentials of Au NPs (1.0 V vs. Ag/AgCl),[37] Ni NPs (above 1.5 V vs. saturated calomel reference electrode)[38] and Cu NPs (0.[illegible] vs.saturated calomel reference electrode).[39]

Table 1. Peak currents (mean ± standard deviation in all cases) measured for separate Ag nanowire and nanoparticle solutions (directly), and for mixtures of the two (by fitting).

Concentration (μg mL^{-1})	Peak current in individual solution (nA)		Fitted peak current in mixture (nA)	
	AgNWs	AgNPs	AgNWs	AgNPs
0.25	65.67 ±18.16		55.15 ±14.19	
10		50.42 ±9.06		50.52 ±12.05
0.10	33.11 ±12.37		40.5 ±10.25	
20		86.80 ±18.80		88.64 ±4.66

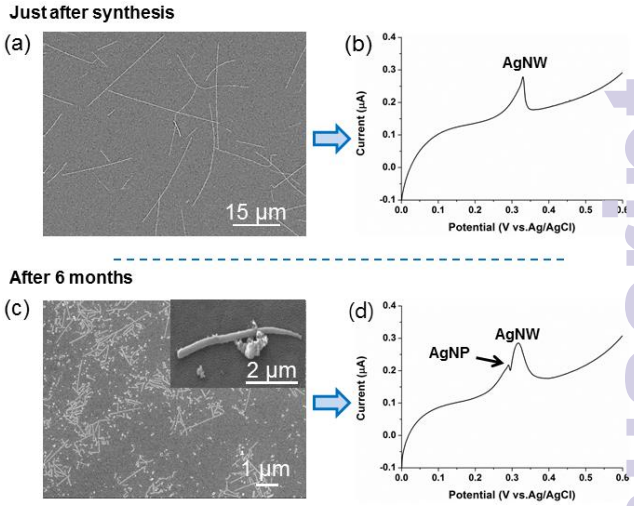

Fig. 3 (a,c) Scanning electron micrographs and b,d) linear swee[illegible] voltammograms (of diluted solutions; scan rate, 20 mV·s^{-1}) measured for Ag nanowire suspensions (a,b) just after synthesis a[illegible] c,d) after 6 months' exposure to air.

Fig. 3a shows a SEM image of Ag NWs in suspension just after synthesis. The NWs are smooth and no NPs are observe[illegible], as confirmed by LSV (Fig. 3b). Fig. 3c, an SEM image of a Ag NW suspension after 6 months' exposure to ambient a[illegible], reveals how the NWs degrade over time, with NPs observed [illegible] the surface of the NWs and in the suspension. Th[illegible] corresponding voltammogram now contains both NW and NP peaks (Fig. 3d). These results show that Ag NWs are unstable [illegible] water. Our method allows their structural integrity to b[illegible] followed over time and the relative proportions of NWs a[illegible] NPs to be monitored. The Ag nanostructures that appear during the synthesis of NWs from NPs can be identified by E[illegible] and spectroscopically (via surface plasmon resonance absorption).[40,41] However, this electrochemical method [illegible] unique in readily allowing the purity of the Ag NWs in the fin[illegible] product to be checked. In addition, the fact that Ag NWs and Ag NPs with same surface capping molecules have their own peak potentials clearly confirms that the difference in the peak position is caused by the different crystal morphologi[illegible] of Ag NWs and Ag NPs.

Recently, Ag NWs have been used to prepare transparent electrodes,[1] for which films of Ag NWs are required. These a[illegible] typically prepared by vacuum filtration, drop casting, or by [illegible] spraying from NW suspensions.[1-5,42] As an example applicati[illegible] therefore, Ag NW films were prepared by vacuum filtratio[illegible] (Fig. 4a), and the NW content of the wastewater wa[illegible] measured by ICP-OES (Fig. 4b) and using our electrochemic[illegible] method (Fig. 4c). The Ag NW concentration measured electrochemically (0.198 μg·mL^{-1}) is in good agreement [illegible] the one obtained by ICP-OES (0.188 μg·mL^{-1}). The averag[illegible] length of AgNWs in the filtrate is below 2 μm (Fig. S1), which is

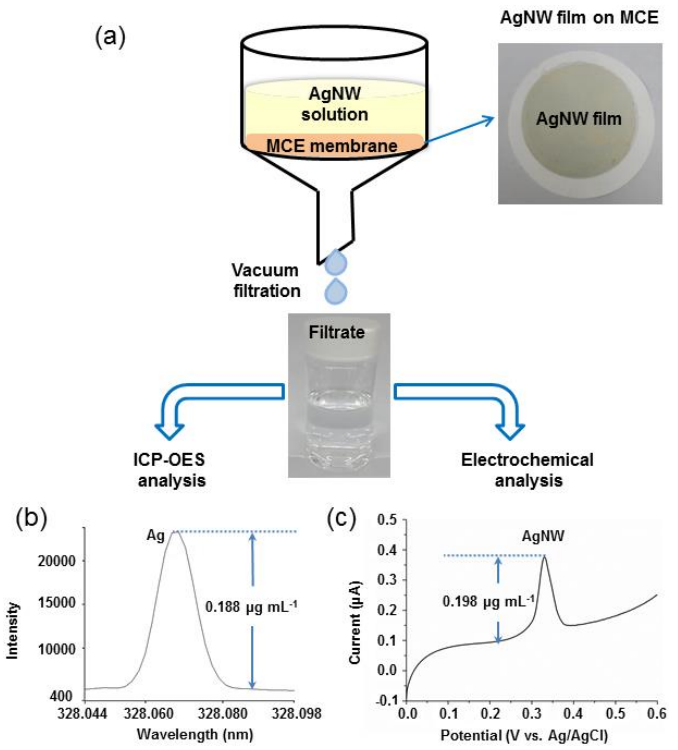

Fig. 4 (a) Schematic of the vacuum filtration setup for the preparation of Ag nanowire films and photographs of the filtrate and of the film on the filtration membrane. (b) ICP-OE spectrum and c) linear sweep voltammogram (scan rate, 20 $mV \cdot s^{-1}$) of the filtrate.

significantly shorter than the Ag NWs in the suspension before the filtration. In spite of the obvious difference in the AgNW length, the current peak potential is not shifted confirming the negligible size effect on the Ag NW quantification. While the electrochemical approach is rapid and portable, ICP-OES requires sample pretreatment with acid and high purity argon gas for detection, making it unsuitable for on-site analysis. Furthermore, it is difficult to separately quantify NPs and NWs in a mixture of the two using ICP-OES.

We have quantified Ag NWs dispersed in DI water by using the electrochemical method. To investigate the interference of ions naturally present in the environmental sample, we used the tap water as an environment sample and monitored Ag NWs in the tap water. Ag NWs were not detected in the unspiked tap water, but a sharp oxidation peak of Ag NWs was obtained for the tap water spiked with Ag NWs showing that the electrochemical method is applicable even for the sample with several ions (Fig. S2a). It should be noted that the oxidation potential was negatively shifted in comparison with that obtained for the Ag NWs in DI water. Previously, it was reported that the presence of chloride ions in the solution causes the negative shift of the potential.[43,44] When we remove Cl^- in the tap water by using a precipitation technique, the oxidation peak returned to its original position (~0.33V) for the case of Ag NWs in DI water (Fig. S2b). Therefore, a pre-filter of Cl^- could be necessary to avoid interference of Cl^- for real environmental samples.

Conclusions

we report the first successful quantifications of Ag NWs in aqueous solution using an electrochemical technique. Ag NWs are identified by the potential of their LSV peak, whose intensity is proportional to their concentration. The low detection limit of this approach makes it ideal to reveal NWs released into water systems. In addition, we relate the crystallographic structure of Ag NWs and NPs to their oxidation potential, showing that differences in their facet structure lead to specific electrochemical potentials. These distinguish Ag NWs and NPs in mixture solutions, allowing their separate quantification. The simple, rapid, and inexpensive method described here could also be employed to rapidly identify other nanomaterials (eg. Au, Ni, and metal oxides) in the human body or in the environment.

Acknowledgements

This work was supported by the Nano Material Technology Development Program (Green Nano Technology Development Program) of the National Research Foundation of Korea (NRF) funded by the Ministry of Science, ICT and Future Planning (No. 2011-0020090). The authors acknowledge Dr. Min Cheol Chu at Korea Research Institute of Standards and Science for his help in measurement of Ag NP size.

Notes and references

1 L. Hu, H. S. Kim, J.-Y. Lee, P. Peumans, Y. Cui, *ACS Nano*, 2010, **4**, 2955.
2 D. Langley, G. Giusti, C. Mayousse, C. Celle, D. Bellet, J.-P. Simonato, *Nanotechnology*, 2013, **24**, 452001.
3 M.-G. Kang, T. Xu, H. J. Park, X. Luo, L. J. Guo, *Adv. Mater.*, 2010, **22**, 4378.
4 P. Lee, J. Lee, H. Lee, J. Yeo, S. Hong, K. H. Nam, D. Lee, S. S. Lee, S. H. Ko, *Adv. Mater.*, 2012, **24**, 3326.
5 L. Li, Z. Yu, W. Hu, C.-h. Chang, Q. Chen, Q. Pei, *Adv. Mater.*, 2011, **23**, 5563.
6 N. K. Verma, J. Conroy, P. E. Lyons, J. Coleman, M. P. O'Sullivan, H. Kornfeld, D. Kelleher, Y. Volkov, *Toxicol. Appl. Pharm.*, 2012, **264**, 451.
7 M. Visnapuu, U. Joost, K. Juganson, K. Künnis-Beres, A. Kahru, V. Kisand, A. Ivask, *BioMed Res. Int.*, 2013, **2013**, 819252.
8 L. D. Scanlan, R. B. Reed, A. V. Loguinov, P. Antczak, A. Tagmount, S. Aloni, D. T. Nowinski, P. Luong, C. Tran, N. Karunaratne, *ACS Nano*, 2013, **7**, 10681.
9 I. G. Theodorou, M. P. Ryan, T. D. Tetley, A. E. Porter, *Int. J. Mol. Sci.*, 2014, **15**, 23936.
10 J. Park, S. Lee, K. Jang, S. Na, *Biosen. Bioelectron.*, 2014, **60**, 299.
11 M. J. Kim, S. Shin, *Food Chem.Toxicol.*, 2014, **67**, 80.
12 E. Bolea, J. Jiménez-Lamana, F. Laborda, J. Castillo, *Anal. Bioanal. Chem.*, 2011, **401**, 2723.
13 C. Cascio, D. Gilliland, F. Rossi, L. Calzolai, C. Contado, *Anal. Chem.*, 2014, **86**, 12143.
14 B. M. Simonet, M. Valcárcel, *Anal. Bioanal. Chem.*, 2009, **393**, 17.
15 R. E. Özel, X. Liu, R. S. Alkasir, S. Andreescu, *TrAC Trend. Anal. Chem.*, 2014, **59**, 112.
16 S. E. Kleijn, S. Lai, M. Koper, P. R. Unwin, *Angew. Chem. Int. Ed.*, 2014, **53**, 3558.

17 K. Scide, J. C. Cuningham, C. Renault, I. Richards, R. M. Crooks, *Anal. Chem.*, 2014, **86**, 6501.
18 M. -P. N. Bui, X. -H. Pham. K. N. Han, C. A. Li, Y. S. Kim, G, H. Seong, *Sensor. Actuat. B*, 2010, **150**, 436.
19 G. Dutta, H. Yang, *Electrochem. Commun.*, 2011, **13**, 1328.
20 Y. -G. Zhou, N. V. Rees, R. G. Compton, *Angew. Chem. Int. Ed.,* 2011, **50**, 4219.
21 S. E. Ward Jones, F. W. Campbell, R. Baron, L. Xiao, R. G. Compton, *J. Phys. Chem. C*, 2008, **112**, 17820.
22 O. S. Ivanova, F. P. Zamborini, *J. Am. Chem. Soc.*, 2010, **132**, 70.
23 H. S. Toh, C. Batchelor-McAuley, K. Tschulik, M. Uhlemann, A. Crossley, R. G. Compton, *Nanoscale*, 2013, **5**, 4884.
24 G. L. Long, J. D. Winefordner, *Anal. Chem.*, 1983, **55**, 712A.
25 H. T. Karnes, G. Shiu, V. P. Shah, *Pharm. Res.*, 1991, **8**, 421.
26 E. Sohn, S. A. Johari, T. Kim, J. K. Kim, E. Kim, J. H. Lee, Y. S. Chung, I. J. Yu. *BioMed Res. Int.*, 2015, **2015**, 893049.
27 J. Mock, M. Barbic, D. Smith, D. Schultz, S. Schultz, *J. Chem. Phys.*, 2002, **116**, 6755.
28 A. Tao, P. Sinsermsuksakul, P. Yang, *Angew. Chem. Int. Ed.*, 2006, **45**, 4597.
29 B. Wiley, Y. Sun, B. Mayers, Y. Xia, *Chem. Eur. J.*, 2005, **11**, 454.
30 C. J. Murphy, A. M. Gole, S. E. Hunyadi, C. J. Orendorff, *Inorg. Chem.*, 2006, **45**, 7544.
31 C. L. Kuo, K. C. Hwang, *Chem. Mater.*, 2013, **25**, 365.
32 J. L. Elechiguerra, L. Larios-Lopez, C. Liu, D. Garcia-Gutierrez, A. Camacho-Bragado, M. J. Yacaman, *Chem. Mater.*, 2005, **17**, 6042.
33 Z. Ni, Z. Wang, L. Sun, B. Li, Y. Zhao, *Mat. Sci. Eng. C*, 2014, **41**, 249.
34 K. Kalimuthu, R. S. Babu, D. Venkataraman, M. Bilal, S. Gurunathan, *Colloid. Surfaces B*, 2008, **65**, 150.
35 Y. Sun, Y. Yin, B. T. Mayers, T. Herricks, Y. Xia, *Chem. Mater.*, 2002, **14**, 4736..
36 Y. Xiong, B. J. Wiley, Y. Xia, *Angew. Chem. Inter. Ed.*, 2007, **46**, 7157.
37 Y. -G. Zhou, N. V. Rees, J. Pillay, R. Tshikhudo, S. Vilakazi, R. G. Compton, *Chem. Commun.*, 2012, **48**, 224.
38 Y. -G. Zhou, B. Haddou, N. V. Rees, R. G. Compton, *Phys. Chem. Chem. Phys.*, 2012, **14**, 14354.
39 B. Haddou, N. V. Rees, R. G. Compton, *Phys. Chem. Chem. Phys.*, 2012, **14**, 13612.
40 S. E. H. Murph, C. J. Murphy, A. Leach, K. Gall, *Cryst. Growth Des.*, 2015, **15**, 1968.
41 K. Kneipp, H. Kneipp, J. Kneipp, *Chem. Sci.,* 2015, **6**, 2721.
42 C.-H. Liu, X. Yu, *Nanoscale Res. Lett.*, 2011, **6**, 75.
43 W. Cheng. E. J. E. Stuart, K. Tschulik, J. T. Cullen, R. G. Compton, *Nanotechnology*, 2013, **24**, 505501.
44 E. J. E. Stuart, K. Tschulik, D. Omanović, J. T. Cullen, K. Jurkschat, R. G. Compton, *Nanotechnology*, 2013, **24**, 444002.